PROCEEDINGS OF SCIENCE

# Time-dependent CP violation in $B^0$ decays

**Seema Bahinipati**[a,*]

[a] *Indian Institute of Technology Bhubaneswar, Bhubaneswar, India*

*E-mail:* seema.bahinipati@iitbbs.ac.in

We present recent measurements of time-dependent charge conjugation-parity (CP) violation (TDCPV) in $B^0$ decays from the Belle II and LHCb experiments. Loop-dominated hadronic penguin decays, which proceed via a $b \to q\bar{q}s$ transition are sensitive to new physics (NP). In the Standard Model (SM), mixing-induced CP violation is suppressed by the polarization of the photon emitted in radiative penguin decays. If there is an NP contribution, there could be a sizable mixing-induced term. TDCPV results from Belle II on $B^0 \to \eta' K^0_S$, $B^0 \to K^0_S K^0_S K^0_S$, $B^0 \to \phi K^0_S$, $B^0 \to K^0_S \pi^0$, $B^0 \to K^0_S \pi^0 \gamma$, and $B^0 \to J/\psi K^0_S$ and only $B^0 \to J/\psi K^0_S$ result from LHCb are presented here.

*16th International Conference on Heavy Quarks and Leptons (HQL2023)*
*28 November-2 December 2023*
*TIFR, Mumbai, Maharashtra, India*

*Speaker





PoS(HQL2023)060

## 1. Introduction

The interference of the decay amplitudes with and without neutral meson mixing can result in charge-parity (CP) symmetry violation in transitions of neutral mesons to CP-invariant final states. CP violation parameters can be precisely measured in an ideal scenario provided by the asymmetric energy of the $e^+e^-$ $B$-factories, as done using Belle II [1] detector at KEKB, Japan and using forward detectors, such as LHCb detector at $p-p$ B-factories, at Large Hadron Collider (LHC), CERN, Switzerland.

Belle II at $e^+e^- \to \Upsilon(4S)$ $B$ factories has high potential to probe CP violation in $B$ mesons. The time interval $\Delta t$ between the decays of two $B$ mesons in an event can be determined thanks to the quantum correlation of the $B^0-\bar{B}^0$ pairs formed during the decay of the $\Upsilon(4S)$ resonance. The initial $B$ meson undergoes a decay that is particular to its flavour, yielding valuable information regarding the flavour of the second B meson. Subsequently, the second $B$ meson undergoes decay into the CP eigenstate. The initial kinematic characteristics of the asymmetric system in the laboratory frame enable the determination of the spatial distance ($\Delta z$) between the decay points of the two $B$ mesons using the existing vertex detectors. The time difference ($\Delta t$) is calculated using the known boost factor from this spatial separation, and fits to $\Delta t$ distribution is used to measure the CP violation parameters.

Although Belle II has a clean environment for CP violation in $B$ mesons, it will be a challenge to search for CP violation in the decay modes with low branching fractions, such as the rare $B_s^0$ meson decays. In addition, LHCb [4] detector operating at the $p-p$ LHC collider has a huge $b\bar{b}$ production cross-section of $\approx 500\ \mu b$, thus, offering an ideal environment for the CP violation studies with the full spectrum of $B$ hadrons.

Mixing-induced CP violation results from the interference between the neutral $B-\bar{B}$ mixing amplitude and the decay amplitude when a neutral $B$ meson decays into a CP-eigenstate ($f_{CP}$). The related CP violation parameters can be inferred from the measurement of the time-dependent decay rates of a $B^0$ and a $\bar{B}^0$ to the specific $f_{\mathrm{CP}}$. The underlying decay-time-dependent CP asymmetry can be expressed as the following ratio, that can expressed in terms of CP violation parameters, namely, $S_{CP}$, and $A_{CP}$:

$$A_{CP} = \frac{\Gamma(\bar{B}^0\to f_{\mathrm{CP}})-\Gamma(B^0\to f_{\mathrm{CP}})}{\Gamma(\bar{B}^0\to f_{CP})+\Gamma(B^0\to f_{\mathrm{CP}})} = Ssin(\Delta m\Delta t) + Acos(\Delta m\Delta t),$$

where $\Delta m$ is the mass difference between the $B^0$ and $\bar{B}^0$ mesons. Here, $A$ is the mixing induced CP violation parameter and $A$ is the direct CP violation parameter ($A = -C$).

## 2. Flavor Tagging

To measure the mixing and CP asymmetries in the decays of neutral $B$-mesons, it is necessary to fully reconstruct a signal $B$ meson, $B_{sig}$, and determine the $b$-flavor of the following $B$ meson, $B_{tag}$. When the two $B$ mesons are entangled, the flavor of $B_{sig}$ at the time of $B_{tag}$ decay is opposite to the flavor of $B_{tag}$. Flavor tagging is the term used to describe this process of determining the flavors of the $B$ mesons.

The objective of the $B$ flavor tagger is to determine the $B_{tag}$ flavor based on the flavor of decay products of $B_{tag}$, without requiring complete reconstruction. Different approaches are used to determine the flavour of the $B$ meson at production. These approaches either use additional particles produced in the $b$ quark's fragmentation associated with the signal-$B$ meson (same side tagging) or use the decay of the $b$ hadron produced in association with the signal (opposite side tagging). For instance, the flavor of a $B$ meson that decays semi-leptonically, $B^0 \to D^{*-} l^+ \nu_l$, can be determined by observing the charge of the charged lepton $l^+$ involved in the decay. The primary inputs for the $B$ flavor tagger are the electric charge and particle identification information of the final state particles. This method of flavar tagging was employed at the predecessor of Belle II experiment, Belle.

The $B$ flavor tagger's output is denoted as $q \cdot r$, where $q$ represents the $B_{tag}$ flavor and $r$ denotes its dilution factor. By convention, flavor content $q = -1$ for $B^0$ and $q = +1$ for $\bar{B}^0$. The dilution factor, denoted as $r$, is determined by the equation $r = 1 - 2w$, where $w$ represents the proportion of incorrectly labeled events. A dilution factor of $r = 0$ signifies the absence of flavor information, whereas $r = 1$ denotes a clear and definite flavor designation.

The probability of a $B$ meson having a flavor content $q$ at some time and decaying to such a CP eigenstate after a time $\Delta t$ is:

$$P(\Delta t, q) = \frac{1}{4 \times \tau_{B^0}} e^{-(\Delta t)/\tau_{B^0}} (1 + q[S_{CP} sin(\Delta m_d \Delta t) + A_{CP} cos(\Delta m_d \Delta t)]),$$

where $S_{CP}$ is the mixing-induced, and $A_{CP}$ the direct CP-violating parameter; $\tau_{B^0}$ is the $b^0$ lifetime; and $\Delta m_d$ is the $B^0 - \bar{B}^0$ oscillation frequency, which corresponds to the mass difference between the two neutral $B$ mass eigenstates.

The usual way to measure how well tagging works is to look at the effective tagging efficiency, which is $\epsilon_{tag} = \epsilon(1 - 2w)^2$, where $\epsilon$ is the averaged $B_{tag}$ reconstruction efficiency. The $\epsilon_{tag}$ quantifies the statistical strength of the dataset, and any enhancement in the tagging accuracy will be manifested in the statistical uncertainty of the CP violation parameters.

At LHCb, similar flavour tagging methods exploit information regarding the additional particles produced in the fragmentation of the $b$ quark associated with the signal-B meson (often called, same side tagging) or from the decay of the $b$ hadron produced in association with the signal (often called, opposite side tagging).

At Belle II, continuous efforts are made to enhance analysis the flavor tagging techniques. A recent advancement is the creation of a novel flavour tagger, named Graph-neural-network Flavor Tagger (GFlaT) [3] that employs all charged particles as decay products of the other $B$ meson and generates a graph structure from these particles. The GFlaT algorithm differs from the previous one by utilizing inter-relational information among particles in the decay of the $B$-tag. The implementation of this novel method has resulted in a significant enhancement of the tagging efficiency $\epsilon_{tag}$, increasing it from $\epsilon_{tag} = (31.68 \pm 0.45 \pm 0.41)\%$ to $\epsilon_{tag} = (37.40 \pm 0.43 \pm 0.34)\%$. The effective tagging efficiency has increased by 18%.

## 3. Belle II and LHCb

The Belle II experiment operates at an asymmetric energy $e^+ - e^-$ collider, SuperKEKB, Tsukuba, Japan, having center of mass energy at $\Upsilon(4S)$ (10.58 $GeV$ resonance). The $e^+$ and $e^-$ energies are 4 GeV and 8 GeV. Belle II is the successor of Belle [1] experiment, that has collected 711 $fb^{-1}$ data sample at $\Upsilon(4S)$ resonance and total of 1 $ab^{-1}$ data during its decade-long running period (1999 - 2010). Belle II started data taking from 2019 and so far it has collected 362 $fb^{-1}$

data sample at $\Upsilon(4S)$ resonance and total recorded data is 424 $fb^{-1}$ till 2022. Belle II aims to collect several $ab^{-1}$ data.

The LHCb experiment operates at the proton-proton collider at CERN accelerator centre located at the Franco-Swiss border, that operates at a center of mass energy at 13.6 $TeV$. LHCb detector is a forward detector that is optimized for $b$ and $c$ meson studies. The major advantages of the LHCb detector are its excellent vertex resolution and particle identification. Belle II has a cleaner environment in comparison with LHCb, as the latter experiment has to deal with events with high multiplicity. About 9 $fb^{-1}$ data has been accumulated by LHCb during its Run 1-2 operation during 2010-2018. Run 3 data-taking started in 2022 with an upgraded detector. LHCb aims to amass a huge cumulative dataset of about 50 $fb^{-1}$ for Run 1-4.

## 4. Recent results from Belle II

This section summarizes the results from Belle II experiment.

### 4.1 $B^0 \to \eta' K^0_S$

Transitions of the type $b \to q\bar{q}s$ are sensitive to NP contributions. The so-called 'hadronic penguin decays' are primarily influenced by a loop diagram, which enables the inclusion of additional contributions from particles outside the SM. $B^0 \to \eta' K^0_S$ is one such decay. The $B^0 \to \eta' K^0_S$ channel exhibits a significant branching fraction compared to other penguin-mediated decays. Furthermore, there exists a precise SM prediction that states the relationship is valid with an accuracy of 1%. The signal candidates in this study are reconstructed utilizing the sub-decay channels $\eta' \to \eta[\to \gamma\gamma]\pi^+\pi^-$ and $\eta' \to \rho[\to \pi^+\pi^-]\gamma$.

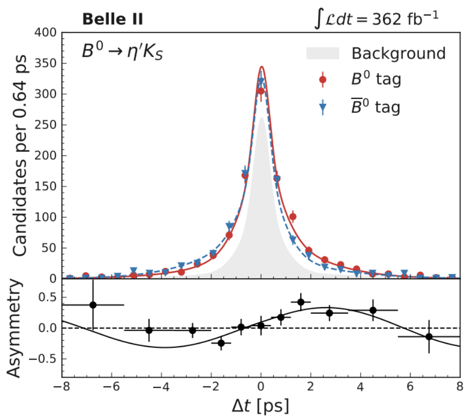


**Figure 1:** Distributions of the proper decay-time difference for $B^0$ and $\bar{B}^0$ tag cases including continuum background (above) and the resulting asymmetry after background subtraction (below).

The primary source of background consists of random combinations of tracks from $e^+e^- \to q\bar{q}(q = u, d, s, c)$ events, often known as continuum background. These are mitigated using a specially trained Boosted Decision Tree (BDT) using event-shape variables. The fitting process consists of two distinct processes. Initially, a multidimensional fit is performed, excluding $\Delta t$, where the majority of parameters for the signal and continuum background shape are allowed to

vary, including yields. During the second phase, only the parameters $S_{CP}$ and $C_{CP}$ are obtained using a multidimensional fit that includes $\Delta t$ in the signal region. The validation of the fit technique is conducted utilizing the control channel, $B^{\pm} \to \eta' K^{\pm}$. Figure 1 shows the plot of the decay time distribution for $B^0 \to \eta' K^0_S$, and the following values of CP violation parameters are obtained:
$S_{\eta' K^0_S} = 0.67 \pm 0.08(stat) \pm 0.03(syst)$,
$C_{\eta' K^0_S} = -0.19 \pm 0.08(stat) \pm 0.03(syst)$ [5].

### 4.2 $B^0 \to K^0_S K^0_S K^0_S$

In the Standard Model (SM), the charmless three-body decay is facilitated by the $b \to sq\bar{q}$ quark transition, which corresponds to a "penguin" one-loop amplitude. The final state of the three-$K^0_S$ system exhibits CP-even behaviour. The decay is characterized by a modest branching fraction of $(6.0 \pm 0.5) \times 10^6$, which is suppressed by the penguin loop. Any enhancement in the observed branching fraction would hint towards NP.

The measurement of decay-time dependent CP violation in $B^0 \to K^0_S K^0_S K^0_S$ decays was done using a data set corresponding to $(198.0 \pm 3.0) \times 10^6$ $B\bar{B}$ pairs collected with the Belle II experiment. Performing this analysis is especially difficult because all reconstructed final-state particles are displaced from the decay vertex of $B^0$. $B$-candidates are reconstructed by combining three $K^0_S$ candidates, which are reconstructed from a pair of oppositely charged pions within a mass window between 0.46 $GeV$ to 0.54 $GeV$. In order to reduce the contamination due to incorrectly reconstructed ("fake") $K^0_S$s, a Boosted Decision Tree (BDT) classifier is used. B candidates are selected using invariant mass of the three $K^0_S$ and beam-constrained-mass $M_{bc}$. A second BDT classifier ($O'_{CS}$) is used for continuum suppression.

Signal yields are extracted for time-differential (TD) and time-integrated (TI) events separately from three-dimensional likelihood fits to the unbinned distributions of $M_{bc}$, $M_{K^0_S K^0_S K^0_S}$ and $O'_{CS}$. Since the kinematic properties of $B^+ \to K^0_S K^0_S K_+$ are similar to those of the signal decay, this mode is used as a control channel. Figure 2 shows the fit projection for $M_{bc}$ for $B^0 \to K^0_S K^0_S K^0_S$ decays, separated into TD and TI samples in the $M_{K^0_S K^0_S K^0_S}$ signal region. The observed mixing-induced CP violation parameters are obtained as [6]: $A_{CP} = 0.07 \pm ^{+0.15}_{-0.20} \pm 0.02$ and $S_{CP} = -1.37 \pm ^{+0.35}_{-0.45} \pm 0.03$.

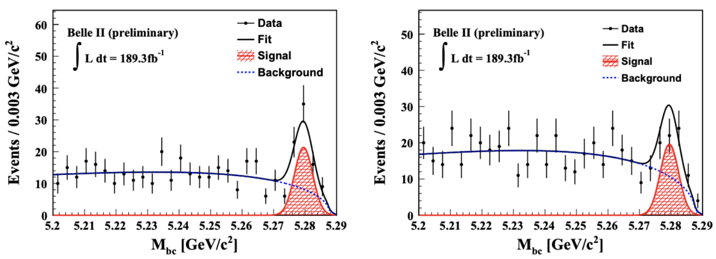


**Figure 2:** Distributions of $M_{bc}$ for (left) TD candidates and (right) TI candidates with fit projections overlaid. The $M_{bc}$ distributions are restricted to events in the $M_{K^0_S K^0_S K^0_S}$ signal region.

### 4.3 $B^0 \to \phi K^0_S$

Previous measurements of CP asymmetries in $B^0 \to \phi K^0_S$ in the Belle and BABAR experiments used time-dependent Dalitz-plot analyses. However, the current Belle analysis [7] employs a quasi-two-body analysis by restricting the sample to candidates reconstructed in a narrow region around the $\phi$ mass, at the cost of a reduced statistical sensitivity. To study CP violating parameters in $B^0 \to \phi K^0_S$ events, a BDT is employed to isolate signal and background events. An extended maximum-likelihood fit is applied to the unbinned distributions of beam-constrained mass, $M_{bc}$, the BDT output, the helicity angle, and the $B$ lifetime to extract the CP violating parameters $A_{CP} = 0.31 \pm 0.20 \pm 0.05$ and $S_{CP} = 0.54 \pm 0.26 \pm ^{+0.06}_{-0.08}$, where the first uncertainties are statistical and the second are systematic [7]. The fit projections onto $\Delta t$ is shown in Fig 3. These results agree with the best measurements on this channel, although dataset is about half that is used in the Belle measurement.

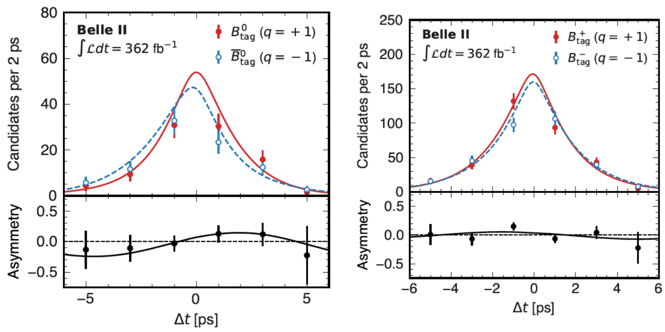


**Figure 3:** Background subtracted projection of fit results onto $\Delta t$ for tagged $B^0$ and $\bar{B}^0$ candidates and the aymmetry for $B^0 \to \phi K^0_S$ (left) and $B^0 \to K^0_S \pi^0$ (right).

### 4.4 $B^0 \to K^0_S \pi^0$

Measurement of the CP-violating parameters, $A_{CP}$ and $S_{CP}$ in $B^0 \to K^0_S \pi^0$ decays at Belle II using integrated luminosity of 362 $fb^{-1}$. These parameters are determined from the difference of the decay-time distributions of $B^0 \to K^0_S \pi^0$ and its charge-conjugate decay. A BDT classifier is used for continuum suppression like in other analysis, yielding a BDT output $C_{BDT}$. An unbinned maximum-likelihood fit to the distributions of $M^{'}_{bc}$, $\Delta t$ and $C^{'}_{BDT}$ is used, where $M^{'}_{bc}$ and $C^{'}_{BDT}$ refer to the transformed variables for $M_{bc}$ and $C_{BDT}$ espectively. A Boosted Decision Tree (BDT) is utilized to separate signal from background events. Figure 4 shows the fit projections onto the time between the decay of the tag-side and signal-side $B$-mesons. The CP-violating parameters $A$ and $S$ are obtained as [8]: $A_{CP} = -0.04 \pm ^{+0.14}_{-0.15} \pm 0.05$ and $S_{CP} = +0.75 \pm ^{+0.20}_{-0.23} \pm 0.04$.

### 4.5 $B^0 \to K^0_S \pi^0 \gamma$

$B^0 \to K^0_S \pi^0 \gamma$ is a radiative penguin decay. The presence of a photon significantly limits the possible variations in the initial state's flavour. Therefore, the final state is not a CP-eigenstate and $S_{CP}$ is inhibited by the helicity of the photon. However, potential NP contributions have the potential to cause a substantial violation of CP through mixing.

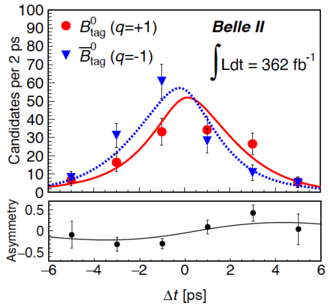


**Figure 4:** Distributions of the proper decay-time difference for tagged $B^0$ and $\bar{B}^0$ after subtracting background

The expected value of the CP-violating observable $S_{CP}$ in the decay process $B^0 \to K^0_S\pi^0\gamma$, as predicted by the Standard Model, is $-0.035 \pm 0.017$ [9]. Due to the relatively short average flight length of the $K^0_S$ before its decay, which is on the order of centimetres, there is no track originating straight from the signal decay vertex in this decay. This analysis is exclusively accessible to Belle II. The process of reconstructing the vertex of the B-meson signal involves combining the momentum of the reconstructed $K^0_S$ particle with a constraint derived from the position of the interaction point and the trajectory of the $B$ meson signal. Candidates exhibiting sub-optimal vertex reconstruction are utilized for the extraction of $C_{CP}$, but are omitted from the time-dependent measurement.

The primary source of background in this analysis arises from simulated photons originating from high-energy $\pi^0$ and $\eta$particle decays. These photons interact with a $K^0_S$ particle and another $\pi^0$ particle to create a signal candidate. An algorithm specifically designed to analyze many variables has been taught to effectively reduce the interference caused by this background. The exclusive decay of $B^0 \to K^{*0}[K^0_S\pi^0]\gamma$ is considered separately than the inclusive decay, $B^0 \to K^0_S\pi^0\gamma$. The corresponding decay time distributions are shown in Figure 5. The CP-violating parameters $C$ and $S$ for the exclusive $B^0 \to K^{*0}(K^0_S\pi^0)\gamma$ decay are obtained as: $C_{CP} = +0.10 \pm 0.13 \pm 0.03$ and $S_{CP} = +0.00 \pm ^{+0.27}_{-0.26} \pm ^{+0.03}_{-0.04}$, and those for the inclusive $B^0 \to K^0_S\pi^0\gamma$ decay are obtained as: $C_{CP} = -0.06 \pm 0.25 \pm 0.07$ and $S_{CP} = +0.04 \pm ^{+0.45}_{-0.44} \pm 0.10$.

### 4.6 $B^0 \to J/\psi K^0_S$

Measurement of the mixing-induced and direct CP violation parameters $S_{CP}$ and $A_{CP}$ from $B^0 \to J/\psi K^0_S$ decays reconstructed by the Belle II experiment is performed using 190 $fb^{-1}$ of integrated luminosity [10].

Figure 6 shows the background subtracted $\Delta t$ distributions of $B^0 \to J/\psi K^0_S$ (left) and $B^+ \to J/\psi K_+$ (right) decays, separated by $B_{tag}$ flavor. The values of CP violation parameters obtained are $S_{CP} = 0.720 \pm 0.062 \pm 0.016$ and $A_{CP} = 0.094 \pm 0.044 + 0.042 - 0.017$, where the first uncertainties is statistical and the second one is systematic.

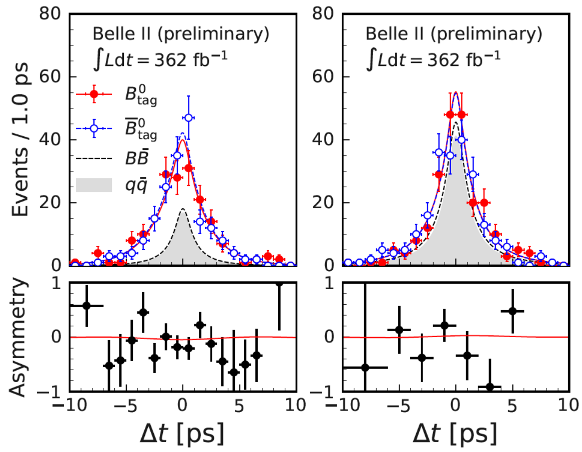


**Figure 5:** Distributions of the proper decay-time difference for tagged $B^0$ and $\bar{B}^0$ including $q\bar{q}$ and $B\bar{B}$ background (above) and the resulting asymmetry after background subtraction (below). The plot for the exclusive decay via $B^0 \to K^0_S \pi^0 \gamma$ is shown on the left, while the inclusive decay is shown on the right.

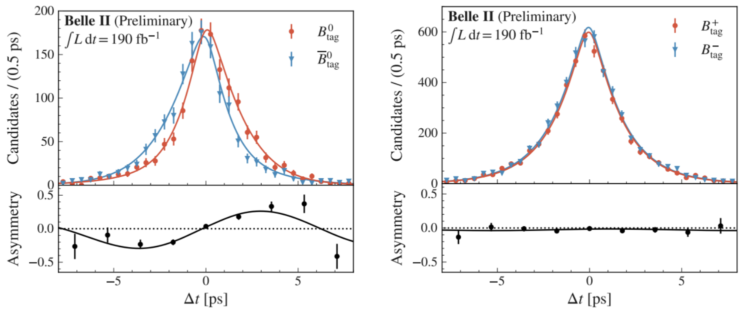


**Figure 6:** Background subtracted $\Delta t$ distributions of $B^0 \to J/\psi K^0_S$ (left) and $B^+ \to J/\psi K_+$ (right) decays, separated by $B_{tag}$ flavor. The fit projections are shown by solid curves and the asymmetry is displayed below the fits.

## 5. Recent results from LHCb

### 5.1 $B^0 \to J/\psi K^0_S$

The decays of $B^0$ and $\bar{B}^0$ mesons to the final states $J/\psi K^0_S$ with $J/\psi \to \mu^+\mu^-$ and $J/\psi \to e^+e^-$, and $\psi(2S)K^0_S$, where $\psi(2S) \to \mu^+\mu^-$ are measured for time-dependent CP violation, using 6 $fb^{-1}$ data recorded at the centre-of-mass energy of $\sqrt{s} = 13\ TeV$ with the LHCb detector [11]. A combined, time-dependent maximum-likelihood fit is performed to measure the CP-violation parameters, with kinematic cuts on the final state particles and dimuon and dielectron invariant masses. $K^0_S$s are reconstructed from the hits in the a silicon-strip vertex locator sub-detector (VELO) as well as by subsequent LHCb tracking detectors. The signal $B^0$ candidates are formed from reconstructed $K^0_S$ and $J/\psi$ candidates forming a good-quality vertex, which is displaced from the primary pp interaction vertex (PV). The background due to random track combinations, named combinatorial background, is reduced with a BDT.

Flavour Tagging (FT) methods that either exploit additional particles produced in the fragmentation of the $b$ quark associated with the signal-B meson (same side tagging) or from the decay of the $b$ hadron produced in association with the signal (opposite side tagging) are used to determine the flavour of the $B$ meson at production. Unbinned, extended maximum-likelihood fits to the invariant-mass distributions of the signal candidates are performed for each final state to determine the signal and background contributions. Figure 7 shows the invariant-mass distribution of the selected candidates with an identified flavour at production of the three signal channels. The CP-violation parameters are measured for the individual modes and a simultaneous fit of the three decay modes is also performed.

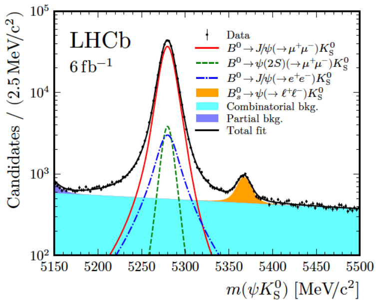


**Figure 7:** Invariant-mass distribution of the selected candidates with an identified flavour at production of the three signal channels.

The measured CP violation parameters are: $S_{J/\psi K^0_S} = 0.717 \pm 0.013(stat) \pm 0.008(syst)$, and $C_{J/\psi K^0_S} = 0.008 \pm 0.012(stat) \pm 0.003(syst)$. The combination of LHCb Run 1 and 2 results is also performed, and the following values of CP-violation parameters are obtained: $S_{\psi K^0_S} = 0.724 \pm 0.014(stat + syst)$, and $C_{\psi K^0_S} = 0.004 \pm 0.012(stat + syst)$,
$S_{J/\psi K^0_S} = 0.726 \pm 0.014(stat + syst)$, and $C_{J/\psi K^0_S} = 0.010 \pm 0.012(stat + syst)$. Figure 8 shows the time-dependent CP asymmetry from the maximum-likelihood estimator of the binned asymmetry with the fit result overlaid. The result of the simultaneous fit to all channels is more precise than the current HFLAV world average [12].

## 6. Summary

Time-dependent CP violation studies in rare $B^0$ meson decays are being conducted in the Belle II and LHCb collaborations. Several novel findings in these domains have been presented from Belle II and LHCb experiments. thanks to its pristine collision environment, Belle II has exclusive access to numerous channels inside the covered decay classes. Furthermore, a number of the most recent Belle II findings are comparable to the most outstanding measurements achieved thus far, and in some cases, even surpass them. With the resumption of data collection in early 2024 and the implementation of advancements in both software and hardware, we anticipate significant improvements in the results obtained from the Belle II experiment in the near future. The huge $b\bar{b}$ production cross-section at LHCb will allow precison meaurements of $CP$ violation in rare $B$

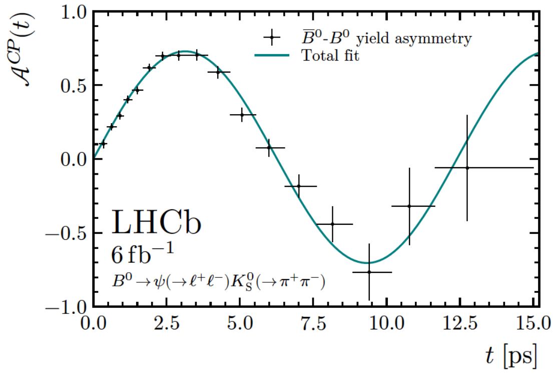


**Figure 8:** Time-dependent CP asymmetry from the maximum-likelihood estimator of the binned asymmetry with the fit result overlaid.

hadron decays using the huge statistics of 50 $fb^{-1}$ that LHCb aims to amass will be able to make significant contribution to $CP$ violation.

## References

[1] Altmannshofer, W. et al., Belle II collaboration, The Belle II Physics Book, BELLE2-PUBPH-2018-001.

[2] LHCb collaboration, A. A. Alves Jr. et al., The LHCb detector at the LHC, JINST 3 (2008) S08005.

[3]

[4] Belle II collaboration, I. Adachi et al., arXiv:2402.17260 [hep-ex].

[5] Oskar Tittel, on behalf of the Belle II collaboration, Recent time-dependent measurements of CP violation at Belle II, PoS (EPS-HEP 2023) 345.

[6] Belle II collaboration, I. Adachi et al., Measurement of decay-time dependent CP violation in $B^0 \to K^0_S K^0_S K^0_S$ using 2019–2021 Belle II data, arXiv:2209.09547v2 [hep-ex].

[7] Belle II collaboration, I. Adachi et al., Measurement of CP asymmetries in $B^0 \to \phi K^0_S$ decays with Belle II, Phys.Rev.D 108 (2023) 7, 072012.

[8] Belle II collaboration, I. Adachi et al., Measurement of CP violation in $B^0 \to K^0_S \pi^0$ decays at Belle II, PRL 131, 111803 (2023), arXiv:2305.07555 [hep-ex].

[9] M. Matsumori, A. I. Sanda, and Y.-Y. Keum, CP asymmetry, branching ratios and isospin breaking effects of $B \to K^* \gamma$ with the perturbative QCD approach, Physical Review D, 72(1).

[10] Belle II collaboration, I. Adachi et al., Measurement of decay-time-dependent CP violation in $B^0 \to J/\psi K^0_S$ decays using 2019-2021 Belle II data, arXiv:2302.12898 [hep-ex].

[11] LHCb collaboration, R. Aaij, *et. al.*, Measurement of CP violation in$B^0 \to \psi(\to l^+l^-)K^0_S(\to \pi^+\pi^-)$ decays, Phys. Rev. Lett. 132 (2024) 021801.

[12] Y. Amhis et al., Averages of $b$-hadron, $c$-hadron, and $\tau$-lepton properties as of 2021, Phys. Rev. D107 (2023) 052008, arXiv:2206.07501, updated results and plots available at https://hflav.web.cern.ch.